

LETTER TO THE EDITOR

Finding binary active galactic nuclei candidates by the centroid shift in imaging surveys

II. Testing the method with SDSS J233635.75-010733.7

Yuan Liu

Key Laboratory of Particle Astrophysics, Institute of High Energy Physics, Chinese Academy of Sciences, PO Box 918-3, 100049 Beijing, PR China
e-mail: liuyuan@ihep.ac.cn

Received 4 March 2016 / Accepted 27 June 2016

ABSTRACT

We have previously proposed selecting binary active galactic nuclei (AGNs) candidates using the centroid shift of the images that is induced by the non-synchronous variations of the two nuclei. In this paper, a known binary AGN (SDSS J233635.75-010733.7) is employed to verify the functioning of this method. Using 162 exposures in the *R* band of the Palomar Transient Factory (PTF), an excess of dispersion in the positional distribution of the binary AGN is detected, although the two nuclei cannot be resolved in the images of PTF. We also propose a new method to compare the position of the binary AGN in PTF *g* and *R* band and find that the difference is highly significant even with only 20 exposures. This new method is efficient for two nuclei with different spectral energy distributions such as type I + type II AGN or an off-set AGN. Large-scale surveys such as the Panoramic Survey Telescope and Rapid Response System, and the Large Synoptic Survey Telescope are expected to discover a large sample of binary AGN candidates with these methods.

Key words. galaxies: active – astrometry – methods: data analysis

1. Introduction

Supermassive black holes (SMBHs) are discovered in the majority of massive galaxies (Kormendy & Richstone 1995). They are thought to have grown through mergers and gas accretion (Volonteri et al. 2003; Di Matteo et al. 2008; Kormendy & Ho 2013). Thus, binary active galactic nuclei (AGNs; binary AGNs are generally defined here as any double sources discovered by imaging or spectroscopy, and we do not strictly distinguish binary AGNs from dual AGNs or AGN pairs) are expected to be common because galaxy mergers can trigger the activity of SMBHs (Begelman et al. 1980; Hernquist 1989; Kauffmann & Haehnelt 2000; Hopkins et al. 2008). Although hundreds of binary AGNs are found with separations of tens of kiloparsec (kpc), only about ten binary AGNs are known with separations ~ 10 kpc (Junkkarinen et al. 2001; Komossa et al. 2003; Hennawi et al. 2006; Fu et al. 2011; Koss et al. 2011; Mazzarella et al. 2012; Liu et al. 2013; Müller-Sánchez et al. 2015). The occurrence rate of kpc-scale binary AGNs ($\sim 1\%$) is lower than the expected value by a factor of ten assuming that each major merger can induce a binary AGN (Yu et al. 2011). Non-simultaneous activity and the gas content of galaxies are invoked to reconcile this apparent discrepancy (Foreman et al. 2009; Yu et al. 2011; Van Wassenhove et al. 2012).

On the observational aspect, a large and complete sample is important to assess this discrepancy. Serendipitously discovered binary AGNs are rare and not sufficient to build a statistically meaningful sample. A systematic method is required for identifying kpc-scale binary AGN candidates. Double-peaked narrow lines (e.g., double-peaked [O III] lines) have been used to select

kpc-scale binary AGNs (Wang et al. 2009; Liu et al. 2010; Smith et al. 2010; Shen et al. 2011). However, double-peaked narrow lines are usually produced by the gas dynamics (Fu et al. 2012; Blecha et al. 2013; Müller-Sánchez et al. 2015). Moreover, the line shift of a binary AGN in a face-on orbit is small and undetectable. Therefore, an efficient method is needed to complement spectroscopy methods.

Liu (2015, hereafter Paper I) showed that the imaging centroid of a binary AGN will shift as a result of the non-synchronous variation of the two nuclei. Thus, these binary AGNs can be revealed by multi-epoch observations even if the separation is smaller than the angular resolution. This method uses the violent variation of AGNs; thus, it is more suitable for two type I AGNs or blazars with strong variability, and its efficiency is low for type I and II binaries. Therefore, we still need an efficient method for the pairs including type II AGN or a galactic nucleus without an AGN. The continuum of type I AGN is bluer than that of type II AGN or a galactic nucleus without an AGN, which is another distinguishable property of AGNs that can be used to uncover binary AGNs. If the spectral energy distributions (SEDs) of two nuclei are significantly different and two or more filters are available, the images of the blue and red filter are more dominated by the bluer and redder nucleus, respectively. As a result, the centroid of the binary in the blue (red) filter should shift toward the bluer (redder) nucleus compared with the centroid in the red (blue) filter. This new method is expected to be valid for two nuclei with different SEDs such as type I and II AGN, type I AGN and a broad absorption line (BAL) quasar, and type I AGN and a galaxy (offset AGN). It is also appropriate for two type II nuclei if the colors of the two

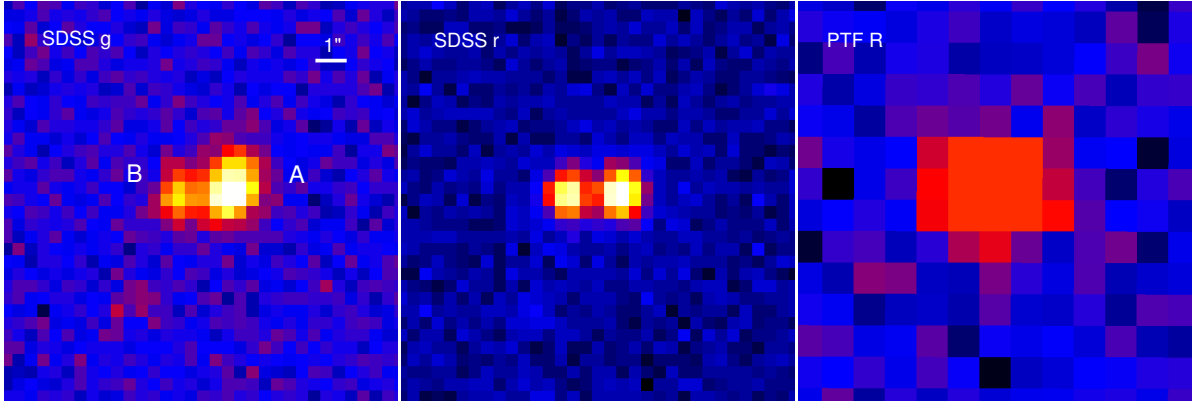


Fig. 1. Images of SDSS J233635.75-010733.7 in SDSS *g* band (left), SDSS *r* band (middle), and PTF *R* band (right). The two nuclei are well resolved in the SDSS images (quasar A is a normal quasar and quasar B is a BAL quasar), but they are blended in the PTF image because of the relatively poor seeing and large pixel scale.

host galaxies are remarkably different. As we mentioned in Paper I, the fast variation in the jet or the reflection from a cloud near a single AGN can mimic another nucleus in the image and thus contaminates the candidates selected by the centroid shift. Follow-up high-resolution imaging and spectroscopy are still required to confirm the candidates. Before hunting for new binary AGNs, we would therefore like to select a known binary AGN to verify the two methods.

In Sect. 2 we describe the target and data selection. In Sect. 3 the procedure for calculation of the centroid in one band is explained. In Sect. 4 the result of the centroid shift between two bands is shown. In Sect. 5 we discuss the implications of the results and present our conclusions.

2. Target and data selection

Since more than 100 exposures are required by the method proposed in Paper I, the Palomar Transient Factory (PTF), with a large sky coverage and frequent exposures, was selected to test our methods. There are three criteria employed to select a known binary AGN covered by PTF: (1) there is at least one type I nucleus in the binary; (2) the two nuclei are not resolved in PTF images; and (3) there are more than 100 exposures to ensure the significance. As a result, only one source, SDSS J233635.75-010733.7, was found to be suitable for testing our method. This source has been discovered by an infrared imaging survey at the Keck Observatory and was confirmed to be a binary quasar (a standard quasar with a blue continuum, broad emission lines, and a BAL quasar) by resolved optical spectra (Gregg et al. 2002). The separation of the two quasars is $1.67''$, while the mean seeing of PTF observations is $2.1''$ and $2.2''$ in *R* and *g* band, respectively. The pixel scale of the PTF CCD is $1.01''$ (Law et al. 2009). Thus, the two quasars cannot be resolved in the image of the PTF (Fig. 1 right), even though the source slightly deviates from the point spread function (PSF). PTF observed this source 162 and 103 times at *R* and *g* band, respectively¹. As a result, this source is appropriate for the test of the centroid method.

3. Centroid shift in *R* band

We present a realistic procedure for the method proposed in Paper I in this section for the *R* band exposures of SDSS J233635.75-010733.7.

¹ <http://irsa.ipac.caltech.edu/applications/ptf/>

The centroids in pixel units of all sources in the 162 *R* band exposures were calculated by SExtractor². The sources with a significance higher than 3σ in at least four adjacent pixels were extracted. The windowed centroids, XWIN_IMAGE and YWIN_IMAGE, were adopted to achieve an accuracy close to the theoretical limit set by the image noise³. The RA and Dec in J2000 were also recorded.

A master frame was selected to define the baseline of positions. Since we only need relative astrometry, the selection of the master frame is arbitrary and our final result is not sensitive to it. In practice, the exposure with a high signal-to-noise ratio (S/N) is preferred to include more reference sources.

The sources around SDSS J233635.75-010733.7 with distances between $20''$ and $180''$ were identified as reference sources. There are 18 reference sources in total. However, some of them may be not available in some exposures with low S/Ns. The centroid of the target quasar in the master frame is noted as X^q and Y^q , and the centroids of the reference sources in the master frame are X_i^r and Y_i^r , where $i = 1-18$.

The centroids of the detected reference sources were adopted to determine the coordinate transformation between every frame and the master frame. A linear transformation is sufficient for small angular scales,

$$X_i^r = a_j + b_j X_{ij}^r + c_j Y_{ij}^r, \quad (1)$$

$$Y_i^r = d_j + e_j X_{ij}^r + f_j Y_{ij}^r, \quad (2)$$

where X_{ij}^r and Y_{ij}^r are the centroids of the i th reference source in j th frame (excluding the master frame). If more than six reference sources are detected in one frame, we can fit Eqs. (1) and (2) to determine the transformation coefficients $a_j \cdots f_j$ of this frame. The frames without sufficient reference sources were discarded. Figure 2 shows an example of the linear fitting.

The residual of the position of reference sources after the transformation determines the astrometric accuracy,

$$x_{ij}^r = X_i^r - (a_j + b_j X_{ij}^r + c_j Y_{ij}^r), \quad (3)$$

$$y_{ij}^r = Y_i^r - (d_j + e_j X_{ij}^r + f_j Y_{ij}^r). \quad (4)$$

² <http://www.astromatic.net/software/sextractor>

³ <https://www.astromatic.net/pubsvn/software/sextractor/trunk/doc/sextractor.pdf>

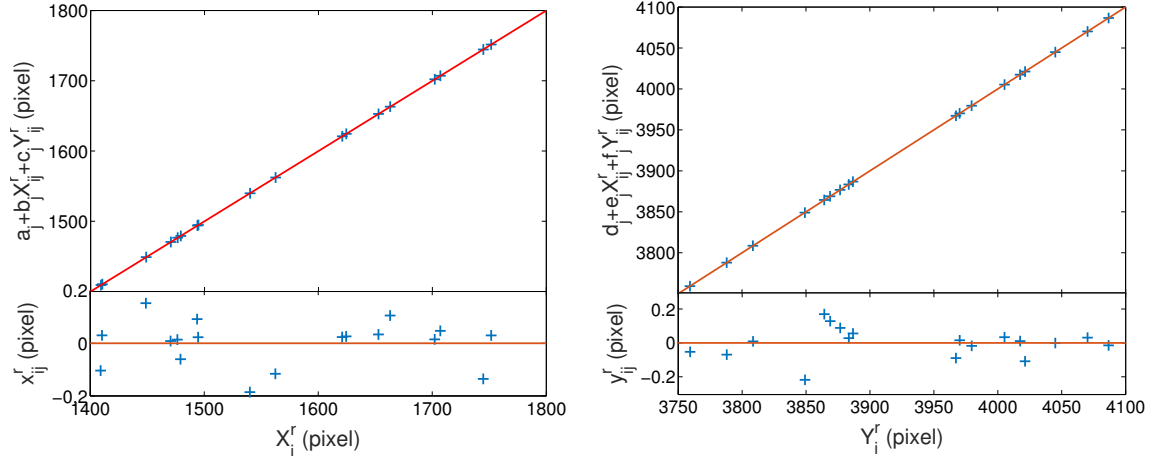


Fig. 2. Example of the linear fitting to determine the transformation coefficient between the master frame and a given frame. The residuals of x and y are scattered around zero under the linear transformation; therefore, no higher order term is included in the current work.

We then calculated the residual of the position of the target quasar in j th frame using the same transformation:

$$x_j^q = X_j^q - (a_j + b_j X_j^q + c_j Y_j^q), \quad (5)$$

$$y_j^q = Y_j^q - (d_j + e_j X_j^q + f_j Y_j^q), \quad (6)$$

where X_j^q and Y_j^q are the centroids of the target quasar in j th frame (excluding the master frame).

We removed the outliers in x_{ij}^r , y_{ij}^r , x_j^q , and y_j^q that deviated from the mean value by more than 4σ . This process was performed iteratively until no new outlier was found. Then the systematic offset in x_j^q and y_j^q was corrected, that is, the means of x_j^q and y_j^q were set to be zero.

The distribution of x_{ij}^r , y_{ij}^r , x_j^q , and y_j^q should be similar if the target quasar is a single AGN. However, the distribution of the residual of a binary AGN should be elongated along the direction of the two nuclei (see the simulations in Paper I). A large astrometric error or a small sample could hide the elongated distribution. Since the direction of the two nuclei is not known a priori, we performed a principle component analysis on x_j^q and y_j^q to determine the direction of the highest dispersion.

Then x_{ij}^r , y_{ij}^r , x_j^q , and y_j^q were projected in the direction of the highest dispersion and the perpendicular direction. The corresponding distributions are noted as \tilde{x}^r , \tilde{y}^r , \tilde{x}^q , and \tilde{y}^q .

A Kolmogorov-Smirnov (K-S) test was used to examine whether these distributions are significantly different. The distribution \tilde{x}^q is expected to be different from the others. We performed K-S tests on three pairs: \tilde{x}^q vs. \tilde{x}^r , \tilde{x}^r vs. \tilde{y}^r , and \tilde{y}^q vs. \tilde{y}^r . The p -values are 0.0075, 0.77, and 0.076, respectively. This shows that the distribution of the residual of the quasar position is indeed different from that of the reference sources in one direction. Furthermore, the standard deviations of \tilde{x}^q , \tilde{y}^q , \tilde{x}^r , and \tilde{y}^r are 0.125, 0.099, 0.085, and 0.089 pixels, respectively, which is consistent with the result of K-S tests.

Figure 3 shows the distribution of \tilde{x}^r , \tilde{y}^r , \tilde{x}^q , and \tilde{y}^q and the direction of \tilde{x}^q . We performed 5000 bootstrap runs from x^q and y^q to estimate the error in the direction of \tilde{x}^q . The angle between the x -axis and \tilde{x}^q is noted as θ . Figure 4 shows the distribution of $\sin\theta$. The mean of $\sin\theta$ is 0.20 and the standard deviation is 0.20. The actual direction of the two nuclei is $\sin\theta = 0.03$; thus, the direction of \tilde{x}^q is consistent with it at 1σ level.

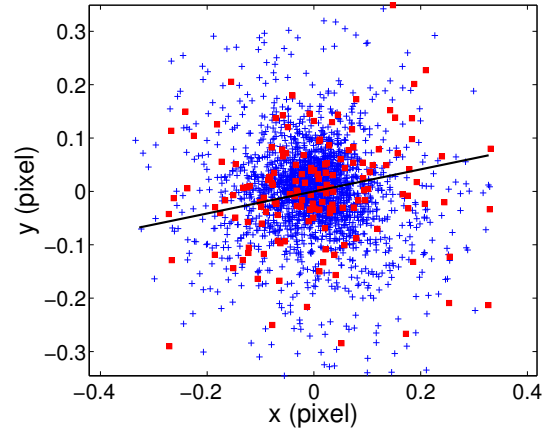


Fig. 3. Distributions of the residual of the position in PTF R band. Squares are the residual of the quasar (x^q and y^q), pluses are the residual of the reference sources (x^r and y^r). The solid line indicates the direction of \tilde{x}^q .

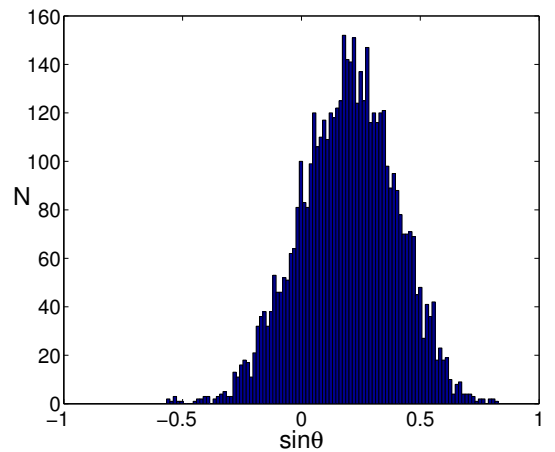


Fig. 4. Distribution of the direction of \tilde{x}^q from 5000 bootstrap runs (see the text in Sect. 3 for details).

4. Centroid shift between R and g band

The method presented in Sect. 3 is appropriate for AGNs with strong variability, that is, for type I AGNs or blazars. In this section, we employ the exposures of R and g band at the same time

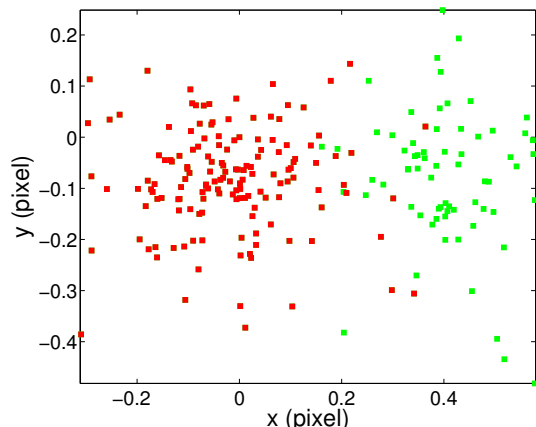


Fig. 5. Comparison between the distribution of the residual of the position in PTF R (red squares) and g (green squares) band. The offset relative to the origin (defined by the mean of the residual of the reference sources) is not corrected because it will not influence the relative positions of the residuals of the two bands.

to alleviate this requirement. According to the optical spectra and SEDs of the two quasars in SDSS J233635.75-010733.7 (Fig. 2 in Gregg et al. 2002), the fluxes of the two quasars are comparable in R band, but the flux of the BAL quasar in g band is lower than that of the blue quasar by a factor of 5 as a result of its intrinsic absorption. Thus, the distribution of the centroids in the two bands should be different. There are only R and g filters in PTF, although the filters with a larger spectral separation could promote the significance.

The same procedures in Sect. 3 were performed on g band using the same reference sources identified in the master frame of the R band.

Figure 5 compares the distributions of the residuals in R and g band. Since the direction of the two nuclei is nearly parallel to the x direction, the residuals in g and R band are expected to be only different in the x direction. The significance indicated by K-S test between the residual in g and R band is 1.6×10^{-39} in the x direction, while the significance is only 0.42 for the y direction. This result is consistent with the visual inspection.

5. Discussion and conclusions

Using a confirmed binary AGN, we have tested the validity of the two centroid methods. Both methods have revealed the signal of two nuclei. The significance of the method using one filter is relatively low (p -value = 0.0075) because the variation of the BAL nucleus is not as strong as the type I nucleus. For the method using two filters, the distributions of the residual in R and g band are significantly different (p -value = 1.6×10^{-39}) and consistent with the expectation from the SEDs of the two quasars. When we randomly selected 20 exposures of R and g band each, the significance of the difference between the distributions of R and g band was still at 10^{-9} – 10^{-6} level. These results indicate the success of the centroid method in uncovering the known binary AGN and its potential power in discovering new binary AGNs.

During the merging process of galaxies, the enhanced inflow may induce strong star formation and significant obscuration. Thus type I+type II or type I+BAL cases should be more common than the type I+type I case (Sanders et al. 1988; Treister et al. 2010). The so-called offset AGNs selected by the multifilter method are also thought to be important tracers of the merging process and valuable for understanding the fueling of AGNs

(Comerford & Greene 2014; Steinborn et al. 2016). However, the multifilter method is not helpful for two type I or II AGNs with similar SEDs.

For the multifilter method, the relative astrometric error between two bands is crucial. Pier et al. (2003) calibrated the astrometry of SDSS images and found that the standard deviation of the distribution of position differences between r filter and other filters is about $0.025''$, which is better than the astrometric error of the r filter against the USNO CCD Astrograph Catalog by a factor of 2. Our method only needs the relative astrometry in arcmin scale and the accuracy should therefore be much better. The distributions of \bar{x}^r and \bar{y}^r in R and g band are well consistent with each other.

A binary system such as SDSS J233635.75-010733.7 is hard to discover by optical spectroscopy because of its high redshift ($z = 1.285$). The commonly employed lines, for example, [O III] and $H\beta$, are already shifted into the infrared band. A large-scale and deep infrared spectroscopy survey of AGNs is still not available at present. However, the centroid methods proposed here are not limited by the redshift in this content if the astrometric error is small enough to identify the centroid shift.

The multifilter method does not require strong variations. Therefore even exposures made in the same night are helpful for identifying the relative shift between different bands. A large sample of binary AGNs may be quickly established by large-scale surveys such as the Panoramic Survey Telescope and Rapid Response System, and the Large Synoptic Survey Telescope.

Acknowledgements. The author thanks the referee for useful comments that clarified the paper. Some data in this work were obtained as part of the Palomar Transient Factory (PTF) project. This work is supported by the National Natural Science Foundation of China under grant Nos. 11573027, 11103019, 11133002, and 11103022.

References

- Begelman, M. C., Blandford, R. D., & Rees, M. J. 1980, *Nature*, 287, 307
 Comerford, J. M., & Greene, J. E. 2014, *ApJ*, 789, 112
 Di Matteo, T., Colberg, J., Springel, V., Hernquist, L., & Sijacki, D. 2008, *ApJ*, 676, 33
 Foreman, G., Volonteri, M., & Dotti, M. 2009, *ApJ*, 693, 1554
 Fu, H., Zhang, Z.-Y., Assef, R. J., et al. 2011, *ApJ*, 740, L44
 Fu, H., Yan, L., Myers, A. D., et al. 2012, *ApJ*, 745, 67
 Gregg, M. D., Becker, R. H., White, R. L., et al. 2002, *ApJ*, 573, L85
 Hennawi, J. F., Strauss, M. A., Oguri, M., et al. 2006, *AJ*, 131, 1
 Hernquist, L. 1989, *Nature*, 340, 687
 Hopkins, P. F., Hernquist, L., Cox, T. J., & Kereš, D. 2008, *ApJS*, 175, 356
 Junkkarinen, V., Shields, G. A., Beaver, E. A., et al. 2001, *ApJ*, 549, L155
 Kauffmann, G., & Haehnelt, M. 2000, *MNRAS*, 311, 576
 Komossa, S., Burwitz, V., Hasinger, G., et al. 2003, *ApJ*, 582, L15
 Kormendy, J., & Ho, L. C. 2013, *ARA&A*, 51, 511
 Kormendy, J., & Richstone, D. 1995, *ARA&A*, 33, 581
 Koss, M., Mushotzky, R., Treister, E., et al. 2011, *ApJ*, 735, L42
 Law, N. M., Kulkarni, S. R., Dekany, R. G., et al. 2009, *PASP*, 121, 1395
 Liu, Y. 2015, *A&A*, 580, A133
 Liu, X., Greene, J. E., Shen, Y., & Strauss, M. A. 2010, *ApJ*, 715, L30
 Liu, X., Civano, F., Shen, Y., et al. 2013, *ApJ*, 762, 110
 Mazzarella, J. M., Iwasawa, K., Vavilkin, T., et al. 2012, *AJ*, 144, 125
 Müller-Sánchez, F., Comerford, J. M., Nevin, R., et al. 2015, *ApJ*, 813, 103
 Pier, J. R., Munn, J. A., Hindsley, R. B., et al. 2003, *AJ*, 125, 1559
 Sanders, D. B., Soifer, B. T., Elias, J. H., et al. 1988, *ApJ*, 325, 74
 Shen, Y., Liu, X., Greene, J. E., & Strauss, M. A. 2011, *ApJ*, 735, 48
 Smith, K. L., Shields, G. A., Bonning, E. W., et al. 2010, *ApJ*, 716, 866
 Steinborn, L. K., Dolag, K., Comerford, J. M., et al. 2016, *MNRAS*, 458, 1013
 Treister, E., Natarajan, P., Sanders, D. B., et al. 2010, *Science*, 328, 600
 Van Wassenhove, S., Volonteri, M., Mayer, L., et al. 2012, *ApJ*, 748, L7
 Volonteri, M., Haardt, F., & Madau, P. 2003, *ApJ*, 582, 559
 Wang, J.-M., Chen, Y.-M., Hu, C., et al. 2009, *ApJ*, 705, L76
 Yu, Q., Lu, Y., Mohayaee, R., & Colin, J. 2011, *ApJ*, 738, 92